NJC

Accepted Manuscript

This is an *Accepted Manuscript*, which has been through the Royal Society of Chemistry peer review process and has been accepted for publication.

Accepted Manuscripts are published online shortly after acceptance, before technical editing, formatting and proof reading. Using this free service, authors can make their results available to the community, in citable form, before we publish the edited article. We will replace this *Accepted Manuscript* with the edited and formatted *Advance Article* as soon as it is available.

You can find more information about *Accepted Manuscripts* in the Information for Authors.

Please note that technical editing may introduce minor changes to the text and/or graphics, which may alter content. The journal's standard Terms & Conditions and the Ethical guidelines still apply. In no event shall the Royal Society of Chemistry be held responsible for any errors or omissions in this *Accepted Manuscript* or any consequences arising from the use of any information it contains.

ROYAL SOCIETY OF CHEMISTRY

www.rsc.org/njc

Cite this: DOI: 10.1039/c0xx00000x

www.rsc.org/xxxxxx

ARTICLE TYPE

Pd(II) complexes with amide-based macrocycles: Syntheses, properties and applications in cross-coupling reactions

Sushil Kumar,[a] Rajeev Ranjan Jha,[a] Sunil Yadav,[a] and Rajeev Gupta*[a]

Received (in XXX, XXX) XthXXXXXXXXX 200X, Accepted Xth XXXXXXXXX 200X

DOI: 10.1039/b000000x

This work shows Pd(II) complexes in a set of 13-membered amide-based macrocyclic ligands varied by the placement of e^-–donating and e^-–withdrawing substituents on the ligand framework. Ligands constitute a N_4 square–planar cavity and optimally house the Pd(II) ion. The solution-state structure via NMR and absorption spectra substantiates the solid-state structure obtained by the crystallography. The electrochemical studies display the impact of electronic substituents on ligands that significantly influence the redox properties and also shift the locus of oxidation. These complexes were used in the Suzuki and Heck cross – coupling reactions. The moderate cross–coupling reaction results are due to limited redox accessibility that can be improved either by using substrates with better leaving group or by placing electron–withdrawing substituents on the macrocyclic ligands.

Introduction

Ligand architecture and its coordination mode in a metal complex plays a significant role in the structural control and redox-regulation of a metal center and therefore reactivity adjustment.[1] Accordingly, understanding ligand architectural parameters that control the structure and redox regulation of a metal ion is crucial and thus systematic study to evaluate structure-redox relationship becomes important. Coordination chemistry with amide-based ligands is of immense interest due to the identification of N_{amide} in several metalloenzymes[2] and prospects of deprotonated N_{amide} group to stabilize higher oxidation state(s) of a metal ion.[3] Out of various amide containing ligands, amide–based macrocyclic ligands are unique as they enforce a geometrically constrained coordination environment around a metal ion.[3a-c,4] Such a constrained environment provides a good opportunity to subtly play with the ligand architecture and evaluate its effect on the structure, redox properties, and reactivity. Our group has been interested to understand the ligand architectural factors that not only affect the structural parameters but also the redox properties.[5] In particular, we have shown that the electronic substituents on ligand have the ability to fine-tune the redox properties of a metal ion and thus its reactivity. Importantly, if electronic substituents are placed on the *o*-phenylene ring which in turn is connected to amidate fragments of a ligand, the effect is quite significant due to the extended conjugation encompassing both metal- and ligand-based orbitals. Noteworthy are the results where we displayed that the locus of the oxidation (metal *versus* ligand) could be varied by a suitable selection of electron–donating or electron–withdrawing substituents on the ligand.[5b,c]

Palladium is an important metal with significant catalytic implications in a variety of organic transformations.[6] The most commonly observed oxidation state is +2 while the catalytic reactions have been suggested to shuttle between 0/+2 states or +2/+4 states.[6a] The palladium complexes in 0, +2 and +4 oxidation states have been well studied.[7] The Pd(I) complexes, while relatively less common, have been employed as pre-catalysts in organic synthesis.[8] By comparison, the coordination chemistry of Pd(III) remains in its infancy.[9] Very few authentic Pd(III) complexes are known and the potential role of Pd(III) ion in catalysis is only now beginning to be elucidated.[9] Schroder and co-workers[10] have shown two structurally characterized homoleptic Pd(III) complexes with S_3- and N_3-based macrocyclic ligands. Recently, Mirica and co-workers[11] have shown a series of octahedral Pd(III) complexes, $[(N_4)Pd^{3+}(X)(Y)]$ (where X/Y = CH_3 and/or Cl), with a pyridine–based N_4 macrocyclic ligand. While the latter report has shown interesting C–C bond formation reactivity of the attached methyl groups; other reports have only postulated the involvement of Pd(III) species in catalysis. Thus, a systematic study has been lacking to relate the catalytic activity to that of structure of palladium complexes. More importantly, delineating the effect of ligand architecture on the redox properties and thus catalytic activities of palladium ion would be an ideal starting point. Herein, we describe four Pd(II) complexes within a set of amide-based macrocyclic ligands where ligands vary by the placement of electronic substituents (–H, –Cl, –Me, and –OMe) on their periphery. These Pd(II) complexes have been explored for their catalytic role in Suzuki and Heck cross–coupling reactions and an attempt has been made to correlate the catalytic observation to that of ligand architecture.

Results and Discussion

Synthesis and Characterization

Complexes **1** – **4** (Scheme 1) were synthesized by treating the respective deprotonated ligand with $Pd(OAc)_2$ followed by standard work-up and recrystallization. All four complexes,

isolated as pale yellow colored crystalline material, were non-electrolytic in nature.[12] Absence of ν_{N-H} stretches and bathochromic shift for the amidic $\nu_{C=O}$ band, compared to free ligand, proves the deprotonated nature of amide group in these complexes.[5c,13] The absorption spectra show features in the UV region thus justifying their pale yellow color. Such spectral features were observed at 300 – 305 nm accompanied by a shoulder between 310 – 337 nm (Figure S1, ESI). Notably, compared to our earlier Ni(II) analogues, d–d transition bands of the present Pd(II) complexes were considerably shifted to shorter wavelength and are located in the UV region (Chart 1, ESI). A similar observation was noted by Lampeka and co-workers[14] for their Ni(II) and Pd(II) complexes of dioxotetramide macrocyclic ligands.

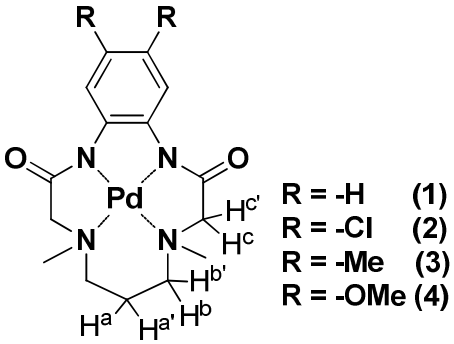

Scheme 1. Chemical drawings of Pd(II) complexes **1** – **4**.

The diamagnetic nature of palladium complexes offered an excellent opportunity to investigate their solution-state structure through proton NMR spectra. Comparative spectra for complexes **1** – **4** are shown in figure S2 whereas table S1 contains the spectral data. In general, ^{1}H NMR spectra of metal complexes of macrocyclic ligands are informative but complex due to the frozen conformation of the chelate rings and a similar situation was observed for the present Pd(II) complexes.[5a-c,i,14,15] The ill–defined multiplets in the upfield region, characteristic of $-CH_2-$ group (protons *a* and *a'*), were observed at *ca.* 1.2 ppm for all four complexes. The resonances observed between 2.5 – 3.0 ppm are assigned to $-CH_2-$ group (protons *b* and *b'*) of trimethylene fragment adopting chair conformation. This results in de-shielding of *axial* protons as compared to *equatorial* protons. Two sets of signals were observed as doublet and triplet at 2.56 and 2.93 for **1**, 2.78 and 3.09 for **2**, 2.57 and 2.98 for **3** and 2.56 and 2.98 for **4**, respectively. The geminal coupling constant $J(H^bH^{b'})$ was found to be between 9.5 – 13.2 Hz. Geminal coupling was also observed for the protons attached to -$C(O)CH_2$- fragment (protons *c* and *c'*). A set of doublets were noted at 3.56 and 4.09 ppm for **1**, 3.60 and 4.00 for **2**, 3.54 and 4.07 for **3** and, 3.55 and 4.11 ppm for **4**, respectively; with geminal coupling constant $J(H^cH^{c'})$ of 15.4–16.1 Hz. Observation of assorted coupling precisely suggests the rigidity of the macrocycle that places various protons to different chemical environment.[5a-c,i,1415] In addition, aromatic ring protons appeared at the most downfield part of the spectrum while a downfield shift was observed on moving from electron-donating to electron-withdrawing group on the arene ring. This clearly reflects electron rich environment of the phenylene ring in the following order: $Cl < H < CH_3 < OCH_3$.

Crystal Structures

The crystal structures of all complexes were determined. The molecular structures are presented in figure 1 whereas selected bond distances and angles are provided in table 1. The structural studies reveal that the Pd(II) ion is bound within the cavity of a macrocyclic ligand while is coordinated by two anionic N_{amide} and two neutral N_{amine} groups. The metal ion is marginally displaced from the N_4 basal plane (0.022–0.037 Å). The Pd(II) ion adopts a distorted square-planar geometry with τ_4 distortion parameter between 0.14 – 0.15.[16] τ_4 has ideal value of 0 and 1 for a perfect square–planar and tetrahedral geometry, respectively. Similar τ_4 distortion parameter of ca. 0.12 was noted for our earlier Ni(II) complexes with identical ligands (Chart 1, ESI).[5c]

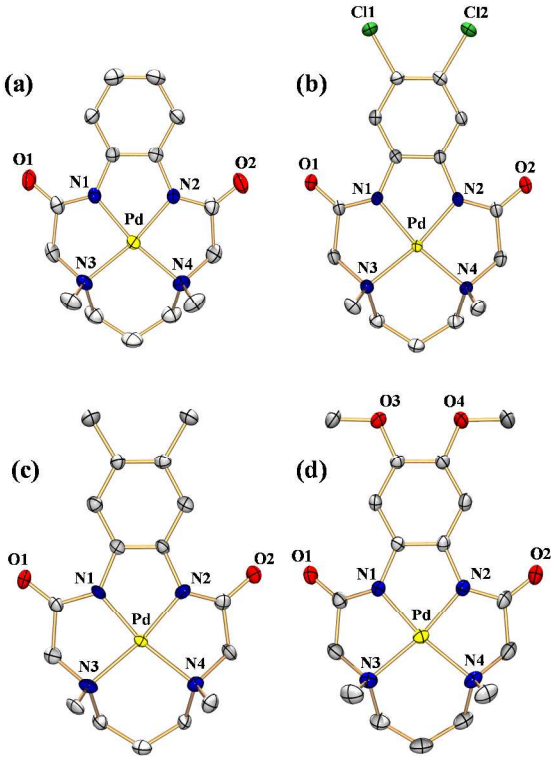

Figure 1. Molecular structures of palladium complexes (a) **1**, (b) **2**, (c) **3** and (d) **4**. Thermal ellipsoids are drawn at 30% probability level while the hydrogen atoms are omitted for clarity.

For complexes **1** – **4**, average Pd–N_{amide} and Pd–N_{amine} bond distances varied within a small window of 1.923 – 1.940 Å and 2.035 – 2.076 Å, respectively. A difference of ca. 0.1 Å between Pd–N_{amide} and Pd–N_{amine} distances is attributed to strong σ donation from anionic N-amidate donors.[5a-c,j] For all four complexes, Pd(II) ion is surrounded by three five-membered chelate rings and one six-membered chelate ring. The N_{amine}–Pd–N_{amine} angle is much larger than that of N_{amide}–Pd–N_{amide} angle due to the involvement of six-membered chelate ring involving two N_{amine} atoms. In all cases, *o*–phenylene ring makes small dihedral angles (2.36–5.51°) and suggests the planarity induced by the aromatic ring. The methyl groups attached to amine nitrogen atoms are situated on the same side, a

feature observed for our earlier nickel and copper complexes with assorted macrocyclic ligands.[5a-c,j] In all cases, six-membered trimethylenediamine chelate ring possesses the typical chair conformation while lateral five-membered chelate rings adopt an envelope conformation.[5a-c,i,j]

All four complexes display interesting solid-state packing due to the involvement of assorted hydrogen bonding, such as CH…O and CH…C, interactions. Such interactions result in the generation of a dimer that further grows either into a chain or a sheet-like network. Notably, presence of these interactions suggests the possibility of stacking of substrates to Pd(II) complexes and such a situation may assist in catalysis. A detailed account of such inetractions has been included in the ESI (Figures S3 – S6 and Table S2).

Table 1. Selected bond lengths (Å), bond angles (°) and τ_4 distortion parameters for complexes **1**, **2**, **3** and **4**.

Bond	$[PdL^{H}]$ (**1**)	$[PdL^{Cl}]$ (**2**)	$[PdL^{Me}]$ (**3**)	$[PdL^{OMe}]$ (**4**)
Bond Lengths				
Pd – N1	1.924(4)	1.938(3)	1.932(8)	1.940(3)
Pd – N2	1.923(3)	1.942(3)	1.913(8)	1.936(3)
Pd – N3	2.043(4)	2.046(3)	2.066(8)	2.058(3)
Pd – N4	2.027(4)	2.044(3)	2.086(9)	2.043(3)
Bond Angles				
N1–Pd–N2	84.86(15)	85.15(12)	83.80(3)	85.13(11)
N1 – Pd – N3	170.13(14)	170.17(12)	170.60(3)	169.80(11)
N1 – Pd – N4	85.65(15)	85.37(12)	85.00(3)	85.49(12)
N2 – Pd – N3	85.35(15)	85.11(12)	86.80(3)	85.01(11)
N2 – Pd – N4	170.45(16)	170.27(12)	168.20(3)	170.61(12)
N3 – Pd – N4	104.11(16)	104.31(12)	104.30(3)	104.34(12)
τ_4	0.138	0.139	0.150	0.139

Electrochemical Studies

To understand the effect of ligand architecture on the electrochemical properties; cyclic voltammetric (CV) and controlled potential electrolysis (coulometry) studies were performed on all Pd(II) complexes. The CV studies were carried out in three different solvents of varying polarity and dielectric constants; DMF, DMSO and MeOH (Table S3, ESI). Complexes **3** and **4** in DMF exhibited reversible redox responses (E_1) at 0.80 and 0.58 V with peak to peak separation (ΔE_p) of 70 and 60 mV, respectively (Figure 2). The remaining two complexes, **1** and **2**, displayed quasi–reversible responses with large ΔE_p values and E_1 potentials of 0.93 and 1.20 V, respectively. The reversibility of E_1 response for complex **4** was maintained in DMSO as well as in CH_3OH with negligible change in potential. A somewhat similar behavior was noticed for complex **3**. However, complexes **1** and **2** only displayed irreversible responses in these two solvents. Along the present series, redox potentials varied based on the type of electron–donating or electron–withdrawing substituents present on the phenylene ring. The potentials decreased in the following order: **2**>**1**>**3**>**4**. The observed trend, not difficult to interpret, is related to the accumulation of electron density at the metal center as a result of electronic substituents.[5b,c] The -OCH_3 groups, being strongest electron–donor, shift the E_1 potential to the lowest in the present case.

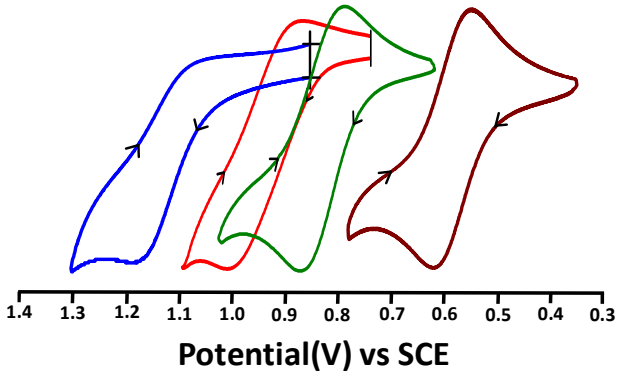

Figure 2. Cyclcic voltammograms of **1** (—), **2** (—), **3** (—), and **4** (—) recorded in DMF.

A comparison of redox potentials of the present Pd(II) complexes with our earlier Ni(II) and Cu(II) complexes (Chart 1 and Table S3, ESI) suggests that the one-electron oxidation potentials for the former are quite positive either from nickel or copper complexes.[5b,c,j] For Pd(II) complexes **1** – **3**, potentials are on the positive side by 0.20 – 0.42 V. This information clearly depicts the inertness of Pd^{2+} state towards one–electron oxidation leading to a Pd^{3+} state. Complex **4**, however, behaves differently and the redox potential is observed at 0.58 V (discussed later). This potential is 150 mV lower than that of nickel analogue and 230 mV when compared to the analogous copper complex. Importantly, electrochemical response for complex **4** was reversible in nature whereas an irreversible response was observed for the analogous nickel and copper complexes.[5b,c,j]

Oxidized Species

One-electron coulometric oxidation of Pd(II) complexes was attempted in DMF to understand the fate of oxidized species. Complexes **1** – **3** afforded transient bright yellow species after one–electron oxidation. The absorption spectra of one–electron oxidized species, $[\mathbf{1}^{Ox}]^+$ – $[\mathbf{3}^{Ox}]^+$, displayed features between 340 – 400 nm (Figure 3). Schroder and co-workers[10] have also noted the generation of a bright yellow color after one-electron oxidation of Pd(II) complex of triazacyclononane ligand. In contrast, a short-lived brownish–green species was resulted after one–electron oxidation of complex **4**. This species displayed distinct absorption spectral features. The spectral maxima were obtained at 580 and 610 nm in addition to broad features between 850 – 1050 nm. The species $[\mathbf{4}^{Ox}]^+$ could also be generated by the stoichiometric oxidation of **4** with $(NH_4)_2[Ce(NO_3)_6]$ either in CH_3OH or DMF. This reaction allowed us to record time – dependent (measured after 0, 5, 15, 30, and 45 seconds) absorption spectra (Figure S7, ESI). As can be seen that $[\mathbf{4}^{Ox}]^+$ was generated immediately after the addition of $(NH_4)_2[Ce(NO_3)_6]$; reached the maximum after 30 seconds; and started decomposing between 30 – 45 seconds.

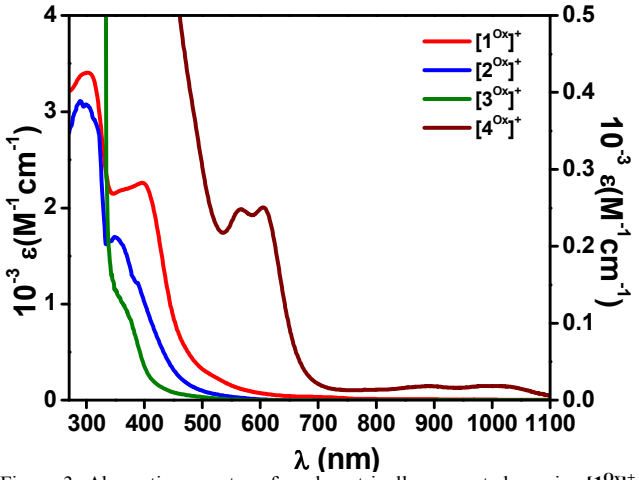

Figure 3. Absorption spectra of coulometrically generated species $[\mathbf{1}^{Ox}]^+$ (—), $[\mathbf{2}^{Ox}]^+$ (—), $[\mathbf{3}^{Ox}]^+$ (—), and $[\mathbf{4}^{Ox}]^+$ (—) recorded in DMF.

EPR spectra of singly-oxidized species were investigated to learn about the true nature of the oxidized species. Notably, $[\mathbf{1}^{Ox}]^+$ – $[\mathbf{3}^{Ox}]^+$ displayed a rhombic EPR spectra suggesting the generation of a Pd(III) species. The observation of three individual g values (ca. 2.026, 2.002, and 1.990) point towards a Pd(III) ion within a square-planar environment. In complete contrast, $[\mathbf{4}^{Ox}]^+$ displayed a sharp isotropic signal at g = 2.011 (ΔH = 18 G) therefore strongly implicating the generation of a radical species (Figure S8, ESI). This suggests that the ligand has lost an electron in case of complex **4**. In fact, absorption spectrum of $[\mathbf{4}^{Ox}]^+$ is dominated by a string of charge-transfer bands which are most likely metal-to-ligand in nature. It is worth to mention that our earlier nickel and copper complexes of similar macrocyclic ligands containing $-OCH_3$ substituents also displayed the generation of ligand-based radicals. Collectively, these results strongly advocate that whenever strong e^--dontaing substituents are present on the macrocyclic ligand; it is the ligand that loses an electron rather than metal.

Thus, we have two sets of complexes: **1** – **3** where oxidation potentially generates Pd(III) species and complex **4** where one-electron oxidation produces a Pd(II)-ligand(+•) species. Importantly, both electrochemical as well as chemical oxidation resulted in identical observation in case of complex **4**. These results prompted us to probe possible organic transformation reactions where redox shuttling of oxidation states of palladium has been proposed. Although, $Pd^{4+/3+}$, $Pd^{2+/+}$ and $Pd^{+/0}$ redox couples were not observed in CV studies; we anticipated that the present complexes will be able to shed light and also distinguish whether a Pd(II)–Pd(III) or a Pd(II)–Pd(II)-ligand(+•) pair can function as a catalyst at all and if yes then which one is a better catalyst. We selected Suzuki and Heck cross-coupling reactions to answer some of the mentioned questions.

Palladium Catalyzed Cross-Coupling Reactions

Several palladium salts and well–characterized complexes have been widely utilized for the synthesis of a variety of chemicals.[6] A facile redox interchange between two oxidation states has been effectively used in the C–X bond formation reactions.[6] The present square-planar Pd(II) complexes supported with dianionic rigid macrocyclic ligands have fairly positive redox potentials; $Pd^{3+/2+}$ couple for **1** – **3** and Pd^{2+}– Pd^{2+}-ligand(+•) for **4**. In addition, $Pd^{4+/3+}$, $Pd^{2+/+}$ and $Pd^{+/0}$ redox couples were not observed. Such facts suggest that the dianionic rigid macrocyclic ligand framework does not support either higher (+4) or lower oxidation states (+1 or 0) of palladium ion. However, the macrocyclic cavity ideally favors the Pd(II) state and transiently supports either Pd(III) or Pd^{2+}-ligand(+•) state. We selected Suzuki[17] and Heck[18] cross-coupling reactions to understand the catalytic effectiveness of the present Pd(II) complexes and to evaluate the influence of electronic groups present on the ligand on the catalytic profile.

Suzuki reaction. Suzuki cross-coupling reaction[17] is a simple yet efficient method for the synthesis of substituted compounds. The catalysis typically involves reaction of aryl or vinyl halide with a suitable boronic acid in presence of a base.[6a] In general, catalyst is either Pd(0) or Pd(II) species whereas the mechanism involves redox interchange between Pd(0) and Pd(II) oxidation states.[6] We attempted coupling reaction of aryl halide with phenylboronic acid in presence of Pd(II) complexes. The reactions were monitored by TLC and/or GC; however products were isolated and characterized in all cases. To identify the most effective reaction conditions, a series of control experiments were performed using 4-methyl bromobenzene and 4-methoxy phenylboronic acid and the results are displayed in table 2.

Table 2. Control experiments for Suzuki cross-coupling reaction between aryl halide and 4-methoxy phenylboronic acid using catalyst **4**.[a]

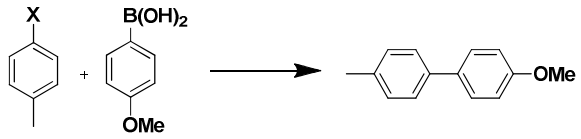

S. No.	X	Base	Catalyst	Product (% yield)
1	Br	-	-	0
2	Br	-	**4**	0
3	Br	Na_2CO_3	-	0
4	Br	Na_2CO_3	$Pd(OAc)_2$	0
5	Br	Na_2CO_3	**4**	62
6	Br	K_2CO_3	**4**	80, 85[b], 85[c]
7	Br	NaOAc	**4**	20
8	Br	K_3PO_4	**4**	15
9	Cl	K_2CO_3	**4**	2, 25[c]
10	I	K_2CO_3	**4**	90

[a]Reaction conditions: DMF:H_2O (4:1), 2 equiv. base, Time 6 h, Temperature 80 ºC, Catalyst: 2 mol%. [b]3 mol%. [c]5 mol%.

It is clear that the reaction between 4-methyl-bromobenzene and 4-methoxy-phenylboronic acid in absence of base and catalyst or in presence of only base or catalyst did not result in any conversion (entries 1-3, table 2). Further, reaction using Na_2CO_3 as the base and $Pd(OAc)_2$ as the catalyst did not results in any yield (entry 4). However, catalyst **4** alongwith Na_2CO_3 displayed 62% conversion (entry 5). Notably, yield increased to 85% with K_2CO_3 as the base (entry 6). On the other hand, alternative bases such as NaOAc and K_3PO_4 (entries 7 and 8) showed poor conversion. Furthermore, 90% yield was acheived using aryl iodide while only 25% prodct formed with

chlorobenzene (entries 9 and 10). It is important to mention that increase in temperature from 80 to 120 ºC did not have a significant effect on conversion. However, increase in catalyst loading from 2 to 3 to 5 mol% did result in higher converstion. Using such optimized conditions, all four catalysts were tested for the cross-coupling reactions between aryl halides and *para*-substituted phenylboronic acid (Table 3). For complex **2**, product yield increased from 35 to 92% on replacing –Cl by –I group on the aryl halide. A similar result was obtained with 4-fluorobenzyloxy boronic acid. The remaining three complexes exhibited similar catalytic performance.

Table 3. Suzuki cross-coupling reaction between tolyl halides and *para*-substituted phenylboronic acid using catalyst **1-4**.[a]

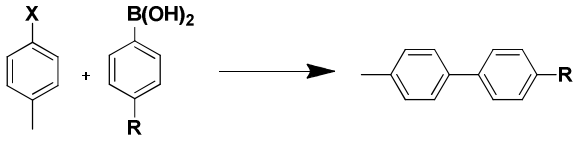

S. No.	R	X	% Yield			
			1	2	3	4
1	OMe	Cl	25	35	12	25
2	4-fluorobenzyloxy	Cl	5	10	5	5
3	OMe	Br	60	90	65	85
4	4-fluorobenzyloxy	Br	50	82	52	78
5	OMe	I	70,70[b]	92	75	90
6	4-fluorobenzyloxy	I	75,73[b]	90	65	85

[a]Reaction conditions: DMF (3 mL), 2 equiv. K_2CO_3 as a base, Time: 6h, Temperature 80 ºC, Catalyst: 5 mol%, [b]Reaction conditions: DMF (2 mL), Time: 15 min., Microwave, Temperature: 80 ºC, Catalyst: 5 mol%.

Heck reaction. Heck reaction[18,19] is also one of the important synthetic tools that allows substitution reaction on planar carbon center. The reaction involves the treatment of halide (typically aryl, vinyl, or benzyl compound) with an alkene (such as acrylate ester or acrylonitrile) in presence of a base to afford the substituted alkene.[6] Heck reaction typically involves oxidation states interplay between Pd(0) and Pd(II) forms. To find out the suitability of our Pd(II) complexes, reactions were carried out between substituted phenyl halide and acrylate esters using complexes **1** – **4** (Table 4). The results are encouraging and follow the similar trend as noted for the Suzuki cross-coupling reactions. On aryl halide, placement of a better leaving group (from -Cl to -I) results in better yield of the product for all four complexes (compare entries 1 – 3, 4 – 6, and 7 – 9). For example, yield increased from 20% to 83% by introducing –I in place of –Cl group for complex **2** whereas 4-methoxyphenyl iodide displayed up to 90% conversion.

Table 4. Heck cross-coupling reaction between *para*-substituted aryl halide and acrylate ester using catalyst **1-4**.[a]

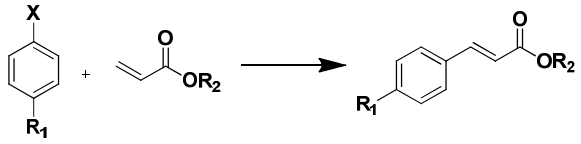

S. No.	R_1	X	R_2	% Yield			
				1	2	3	4
1	Me	Cl	*n*-Bu	10	20	5	15
2	Me	Br	*n*-Bu	30	70	25	68
3	Me	I	*n*-Bu	60, 60[b]	83,82[b]	55,54[b]	75,75[b]
4	OMe	Cl	*n*-Bu	12	25	6	18
5	OMe	Br	*n*-Bu	33	80	26	72
6	OMe	I	*n*-Bu	64	90	64	84
7	OMe	Cl	Me	18	30	10	24
8	OMe	Br	Me	33	75	28	70
9	OMe	I	Me	62	83	55	78

[a]Reaction conditions: DMF (4 mL), 2 equiv. K_3PO_4 as base, Catalyst: 5 mol%, Time: 6h, Temperature: 120 ºC. [b]Reaction conditions: DMF (2.5 mL), 2 equiv. K_3PO_4 as base, Catalyst: 5 mol%, Time: 15 min., Microwave, Temperature: 120 ºC.

Heck coupling using aryl halides with *para*-substituted stryrenes provided an option to understand the stereo-selectivity[20] with the present Pd(II) complexes (Table 5). Typically, such a reaction affords both *cis* as well as *trans* product in variable proportions.[20] Although present Pd(II) complexes provided *trans* isomer as the major product; kinetically favorable *cis* isomer was also obtained in decent amount reaching to 20% in a few cases. We tentatively suggest that a planar Pd-macrocyle is able to interact with styrene and aryl halide simultaneously thus affording kinetically-controlled product. Such examples nicely illustrate the significance of designed coordination complexes in metal-mediated catalysis. As anticipated, employing –I in place of –Br or –Cl (entries 1-3, Table 5) increases the yield without compromising *cis*/*trans* ratio. In addition, presence of electron-withdrawing group on aryl halide provided higher yield of the product whereas presence of electron-withdrawing or electron-donating substituent on styrene did not cause much difference. The reaction most probably proceeds first via the formation of an arylpalladium intermediate, which then reacts with an olefinic compound via addition and then finally undergoes β-hydride elimination of palladium hydride to afford the final product.[20b]

Table 5. Heck cross-coupling reaction between *para*-substituted aryl halide and *para*-substituted styrene using catalyst **1-4**.[a]

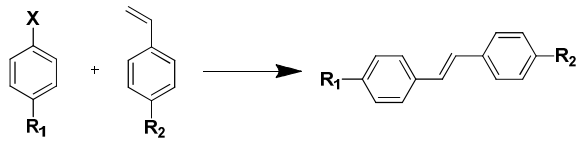

S. No.	R_1	X	R_2	% Yield (*trans* : *cis*)			
				1	**2**	**3**	**4**
1	H	Cl	H	23:2	30:4	28:5	20:1
2	H	Br	H	45:4	85:7	80:9	41:1
3	H	I	H	56:2	83:16	88:8	46:2
4	H	Br	OMe	62:6	74:14	66:6	44:4
5	H	Br	Cl	52:5	57:10	65:5	45:4
6	H	Br	Me	54:5	77:8	68:8	48:3
7	Me	Br	H	59:2	77:8	65:8	39:2
8	*t*-Bu	Br	H	42:2	62:8	60:6	30:1
9	OMe	Br	H	52:2	70:7	56:11	35:1
10	NO_2	Br	H	74:4	90:10	89:7	60:3
11	Me	Br	OMe	65:8	80:20	63:4	56:3
12	OMe	Br	OMe	48:2	68:5	61:5	34:1
13	*t*-Bu	Br	OMe	39:1	60:8	42:15	22:1
14	NO_2	Br	OMe	76:3	92:8	60:5	52:2
15	OMe	Br	Cl	65:5	92:7	79:9	62:1
16	Me	Br	Cl	42:3	62:10	49:10	31:1
17	*t*-Bu	Br	Cl	40:2	60:8	61:6	23:1
18	NO_2	Br	Cl	80:5	90:10	84:15	60:6

[a]Reaction conditions: DMF (4 mL), 2 equiv. K_3PO_4 as base, Catalyst: 5 mol%, Time: 6h, Temperature: 120 ºC. The ratio of *trans:cis* isomers was calculated by GC and verified by proton NMR spectra of isolated products in several cases.

While comparing the effectiveness of four Pd(II) complexes, it is apparent that the yields are higher with complex **2**. We believe that the presence of electron-withdrawing –Cl groups makes the macrocycle and therefore palladium center electron-deficient. Such a situation disfavors the removal of electron(s) either from the metal or ligand and thus disfavors the generation of a potentially high-valent complex. This point is well supported by the observation of E_1 potential at the most positive value for complex **2** out of four Pd(II) complexes.

Notably, after the completion of the Suzuki or Heck reactions, there was no observation of Pd(0) state that is usually encountered as the brown–black insoluble material. We also performed the Hg drop test[21] to further rule out the involvement of Pd(0) state. Thus, when Pd(II) complexes **1 – 4** were used for the Heck coupling between iodobenzene and styrene in presence of a drop of mercury(0); there was no change in the overall product profile as identical results were obtained as noted in entry 3 of Table 5. To further rule out the possibility of the generation of Pd nanoparticles; all four complexes were recovered in nearly quantitative yield after the catalysis and characterized. The recovered Pd(II) complexes displayed superimposable FTIR and NMR spectra to that of pristine samples. Furthermore, all four recovered Pd(II) complexes were able to carry out both the Suzuki as well as the Heck coupling reactions without any loss of catalytic activity.[22] Collectively, these experiments firmly support that the present Pd(II) complexes function as the *true catalysts* and not as the pre-catalysts or generate some other species (such as Pd nanoparticles) that actually carries out the catalysis.

Finally, to ascertain whether the leached [Pd] (Pd nanoparticles or Pd(0) form] is actually functioning as the catalyst; complex **2** was utilized as a representative catalyst for the Heck coupling between iodobenzene and styrene. Thus when complex **2** was removed after 160 min. of the reaction while the reaction was allowed to continue; there was practically no increase in the product formation (Figure 4). After 140 min., complex **2** was added to the reaction mixture, and it was found that there is a sudden increase in the yield of the product. An overall reaction profile exhibits that on removing **2** catalysis was practically ceased while re-adding **2** to the reaction mixture has restarted it. This simple test further establishes the catalytic behavior of complex **2** and confirms that the leached [Pd] is not responsible for the observed catalysis.

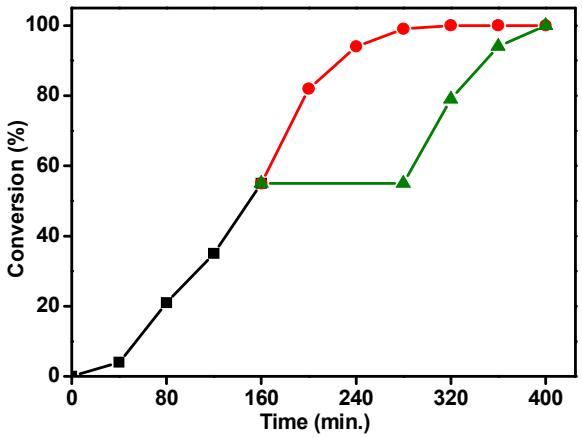

Figure 4. Heck coupling reaction between iodobenzene and styrene in presence of complex **2** showing maximum conversion at 360 min. (red spheres). The complex **2** was removed after 160 min. and the reaction was ceased (black squares). The complex **2** was re-added at 300 min. and the reaction was restarted (green triangles). In all cases, total conversion (*cis* + *trans* products) was calculated using GC. Reaction conditions are as mentioned in Table 5.

The inference that can be drawn from catalysis is that the present Pd^{2+} complexes supported with amide-based macrocycles have the potential to carry out cross–coupling reactions. Although results are moderate; the absence of Pd(0) during the catalysis and electrochemical observation of Pd(III) or Pd^{2+}-ligand(+•) species suggest the possible involvement of $Pd^{3+/2+}$ or Pd^{2+}-ligand$^{(+\bullet)/2+}$ cycle in catalysis. The moderately successfull cross–coupling reactions point toward the sluggishness of catalysis due to only possible one-electron cycle in contrast to two-electron $Pd^{4+/2+}$ and/or $Pd^{2+/0}$ cycles.[6,9] We suggest that the rigidity of the macrocycle is unable to support the desirable geometry preferred by a Pd(0,I)[7,8] or Pd(IV) center.[19] Notably, however, the catalytic efficiency can be improved either by using substrates with better leaving group or by placing electron–withdrawing substituents on the macrocyclic ligands. Such informations may help in better design of the effective catalysts in future.

Conclusions

This work has shown the coordination chemistry of palladium ion in a set of 13-membered amide-based macrocyclic ligands. The solution-state structures, delineated by NMR and absorption spectra, supported the solid-state crystallographic structures. The electrochemical studies displayed that the electronic substituents present on the macrocyclic ligands shift the locus of oxidation from metal (in **1** – **3**) to ligand (in **4**). The axially exposed metal surface of the square–planar Pd(II) complexes and the accessible $Pd^{3+/2+}$ or Pd^{2+}-ligand$^{(+\bullet)/2+}$ redox couple was used to show Suzuki and Heck reactions. The moderate cross–coupling reaction results were due to limited redox accessibility that can be improved either by using substrates with better leaving group or by placing electron–withdrawing substituents on the macrocyclic ligands.

Experimental

Materials and physical measurements. All reagents were obtained from the commercial sources and used as received. The solvent were purified and/or dried following standard procedures.[23] The ligands H_2L^H, H_2L^{Cl}, H_2L^{Me} and H_2L^{OMe} were synthesized according to our earliar report.[5c] The conductivity measurements were done in organic solvents using the digital conductivity bridge from the Popular Traders, India (model number: PT – 825). The micro analytical data were obtained from the ElementarAnalysen System GmbH Vario EL-III instrument. The infra-red spectra were recorded using either Perkin–Elmer FTIR 2000 or Spectrum–Two spectrometer. The absorption spectra were recorded with the Perkin–Elmer Lambda–25 spectrophotometer. NMR spectra were obtained from the Jeol 400 MHz spectrometer. Cyclic voltammetric experiments were performed using a CH Instruments electrochemical analyzer (Model 1120A). The cell contained a glassy-carbon or a platinum working electrode, a Pt wire auxiliary electrode, and a saturated calomel electrode (SCE) as the reference electrode. For coulometric experiments, a Pt mesh was used as the working electrode. The solutions were ~1 mM in complex and ~0.1 M in supporting electrolyte, TBAP. Under our experimental conditions, the $E_{1/2}$ value (in Volts) for the couple Fc^+/Fc in DMF was obtained at 0.47V vs. SCE.[24] Gas chromatography was performed with Clarus 580 Perkin Elmer instrument.

Crystallography. Single crystal X-ray diffraction intensities for complexes **1** – **4** were collected at 293K on an Oxford XCalibur CCD diffractometer equipped with either graphite monochromatic Mo-Kα radiation (λ = 0.71073 Å) or Cu-Kα radiation (λ = 1.54184 Å).[25] The multi-scan absorption correction was applied using CrysalisPRO.[25] The structures were solved by the direct methods using SIR-92[26] and refined by full-matrix least-squares refinement techniques on F^2 using SHELXL97.[27] The hydrogen atoms were placed into the calculated positions and included in the last cycles of the refinement. All calculations were done using WinGX software package.[28] Although, intensity data for complex **2** was collected against the best crystal, due to the poor crystal quality, data completeness remained below 90%. Due to this reason, checkcif file shows a few A level alerts. Crystallographic data collection and structure solution parameters for complexes **1** – **4** are provided in table S4. CCDC numbers 848812 – 848815 contain the supplementary crystallographic data for this paper. These data can be obtained free of charges from The Cambridge Data Center via www.ccdc.cam.ac.uk/data_request/cif.

Synthesis

[PdL^H] (1). Ligands H_2L^H (0.10 g, 0.34 mmol) was dissolved in 10 ml DMF under magnetic stirring and treated with solid NaH (0.018 g, 0.75 mmol) under inert atmosphere. The resulting mixture was stirred till the effervescence was seized. $Pd(OAc)_2$ (0.077 g, 0.34 mmol) dissolved in 5 ml DMF was added drop-wise to the aforementioned reaction mixture. The resulting pale brown solution was stirred for 2h at room temperature. The solvent was removed under reduced pressure and the crude product was isolated after washing with diethyl ether. The crude compound was dissolved in CH_3OH and passed through a pad of celite in a medium porosity frit. The resulting filtrate was concentrated to 1/3rd of its original volume and vapor diffusion of diethyl ether afforded crystalline product within 2 – 3 days. Yield: 0.078g (58%). $C_{15}H_{22}N_4O_3Pd$ (including one H_2O, 412.78): calcd. C 43.65, H 5.37, N 13.57; found C 43.22, H 5.19, N 13.32. IR (KBr disk) 3432 (O-H), 2916 (C-H), 1619 (C=O), 1572 (C=C), 1475 (C=C) cm^{-1}. Conductivity (DMF, ~1 mM solution, 298 K): Λ_M = 5 Ω^{-1}cm^{2}mol^{-1}. UV/Vis [λ_{max}, nm (ε, M^{-1}cm^{-1})] (in DMF): 293 (30210), 310 (sh, 21000). ^{1}H NMR spectrum [400 MHz, $CDCl_3$, 25°C] δ : 1.23 (s, 2H, -CH_2-), 2.56 (d, 2H, -CH_2-, J = 13.20 Hz), 2.75 (s, 6H, -CH_3), 2.93 (t, 2H, -CH_2-, J = 11.72 Hz), 3.56 (d, 2H, -CH_2C(O)-, J = 15.36 Hz), 4.09 (d, 2H, -CH_2C(O)-, J = 16.12 Hz), 6.83 (dd, 2H, Ar-H, J = 5.86 Hz), 8.10 (dd, 2H, Ar-H, J = 5.86 Hz) ppm.

[PdL^{Cl}] (2). A similar procedure as that of complex **1** was adopted for the synthesis of complex **2**. Following reagents were used: H_2L^{Cl} (0.10 g, 0.28 mmol); NaH (0.015 g, 0.61 mmol); $Pd(OAc)_2$ (0.062 g, 0.28 mmol). Yield: 0.066g (53%). $C_{15}H_{18}N_4O_2Cl_2Pd$ (463.66): calcd. C 38.86, H 3.91, N 12.08; found C 39.09, H 4.12, N 12.44. IR (KBr disc) 2923 (C-H), 2854 (C-H), 1627 (C=O), 1560 (C=C), 1467 (C=C) cm^{-1}. Conductivity (DMF, ~1 mM solution, 298 K): Λ_M = 6 Ω^{-1}cm^{2}mol^{-1}. UV/Vis [λ_{max}, nm (ε, M^{-1}cm^{-1})] (in DMF): 301 (11610), 335 (sh, 5080).^{1}H NMR spectrum [400 MHz, $CDCl_3$, 25°C] δ : 1.27 (m, 2H, -CH_2-), 2.78 (d, 2H, -CH_2-, J = 9.52 Hz), 2.80 (s, 6H, -CH_3), 3.09 (t, 2H, -CH_2-, J = 12.44 Hz), 3.60 (d, 2H, -CH_2C(O)-, J = 16.12 Hz), 4.0 (d, 2H, -CH_2C(O)-, J = 15.40 Hz), 8.16 (s, 2H, Ar-H) ppm.

[PdL^{Me}] (3). This complex was also synthesized in a similar manner as mentioned for complex **1** with the following reagents: H_2L^{Me} (0.10 g, 0.31 mmol); NaH (0.016 g, 0.69 mmol); $Pd(OAc)_2$ (0.07 g, 0.31 mmol). Yield: 0.074g (56%). $C_{17}H_{24}N_4O_2Pd$ (422.82): calcd. C 48.29, H 5.72, N 13.25; found C 48.14, H 6.10, N 13.67. IR (KBr disc) 2920 (C-H), 1618 (C=O), 1593 (C=C), 1486 (C=C), 1465 (C=C) cm^{-1}. Conductivity (DMF, ~1 mM solution, 298 K): Λ_M = 10 Ω^{-1}cm^{2}mol^{-1}. UV/Vis [λ_{max}, nm (ε, M^{-1}cm^{-1})] (in DMF): 288 (7170), 294 (7160), 353 (sh, 3230).^{1}H NMR spectrum [400 MHz, $CDCl_3$, 25°C] δ : 1.22 (s, 2H, -CH_2-), 2.13 (s, 6H, Ar-CH_3), 2.57 (d, 2H, -CH_2-, J = 12.48 Hz), 2.75 (s, 6H, -CH_3), 2.98 (t, 2H, -CH_2-, J = 13.20 Hz), 3.54 (d, 2H, -CH_2C(O)-, J = 15.40 Hz), 4.07 (d, 2H, -CH_2C(O)-, J = 15.36 Hz), 7.88 (s, 2H, Ar-H) ppm.

[PdL^{OMe}] (4). A similar procedure as that of complex **1** was adopted for the synthesis with following reagents: H_2L^{OMe} (0.10 g, 0.28 mmol); NaH (0.016 g, 0.62 mmol); $Pd(OAc)_2$ (0.064 g, 0.28 mmol). Yield: 0.066g (51%). $C_{17}H_{24}N_4O_4Pd$ (454.82): calcd. C 44.89, H 5.32, N 12.32; found C 44.77, H 5.48, N 12.12. IR (KBr disc) 2925 (C-H), 1603 (C=O), 1583 (C=C), 1493 (C=C), 1445 (C=C) cm^{-1}. Conductivity (DMF, ~1 mM solution, 298 K): $\Lambda_M = 4\ \Omega^{-1}cm^2mol^{-1}$. UV/Vis [$\lambda_{max}$, nm ($\varepsilon$, $M^{-1}cm^{-1}$)] (in DMF): 296 (33050), 329 (sh, 18650).^{1}H NMR spectrum [400 MHz], $CDCl_3$, 25˚C] δ : 1.23 (s, 2H, -CH_2-), 2.56 (d, 2H, -CH_2-, J = 13.16 Hz), 2.75 (s, 6H, -CH_3), 2.98 (t, 2H, -CH_2-, J = 12.48 Hz), 3.55 (d, 2H, -$CH_2C(O)$-, J = 16.12 Hz), 3.81 (s, 6H, Ar-OCH_3), 4.11 (d, 2H, -$CH_2C(O)$-, J = 15.40 Hz), 7.81 (s, 2H, Ar-H) ppm.

General Procedure for the Suzuki reaction. In a vacuum oven dried tube, required palladium complex, 2 equiv. of K_2CO_3, 1.2 equiv. of boronic acid were dissolved in 2 ml mixture of (4:1) DMF:water. The mixture was degassed under N_2 atmosphere followed by the addition of 1 mmol of aryl halide. The reaction mixture was heated at 80 ˚C either on an oil-bath or in microwave (CEM Discover Benchmate, USA) at 250W power for 15 min. The progress of the reaction was monitored by TLC at regular intervals. After cooling, the mass was diluted with H_2O and extracted with ethyl acetate. The organic layer was separated and dried over Na_2SO_4 followed by the removal of solvent under reduced pressure. The organic products were purified by the column chromatography using silica gel (100-200 mesh) with 5% ethylacetate/hexanes mixture. The products were identified and quantified by NMR spectroscopy as well as by gas chromatography. However, in most cases, the products were isolated and characterized. The spectral data for a few representative products are provided herewith while the spectral figures are collected in ESI (Figures S10–S23).

General Procedure for the Heck reaction. In a vacuum oven dried tube, 2.0 equiv. of K_3PO_4 and required palladium complex were taken in DMF (2 ml). The resulting solution was flushed with N_2 followed by the addition of 1.0 mmol of aryl halide and 1.5 mmol of butyl acrylate. The reaction mixture was heated on an oil bath or under MW (CEM Discover Benchmate, USA) for 15 min at 120 ˚C. The progress of the reaction was monitored by TLC. After cooling, the reaction was quenched with H_2O and the organic products were extracted with ethyl acetate. The organic layer was separated and dried over Na_2SO_4 followed by the removal of solvent under reduced pressure. The organic products were purified on silica gel (100-200 mesh) eluted with 5% ethyl acetate/hexanes mixture. The products were identified and quantified by NMR spectroscopy as well as by gas chromatography. However, in most cases, the products were isolated and characterized. The spectral data for a few represntative products are provided herewith while the figures are collected in ESI (Figures S10–S23).

Spectral data for a few representative products.

Butyl-3-*p*-tolylacrylate.[29,30] The product was obtained as colorless oil. δ_H NMR (300 MHz, $CDCl_3$) 7.65 (1 H, d, J = 15.9 Hz, ArC*H*=CH), 7.42 (2 H, d, J = 7.8 Hz, Ar*H*), 7.18 (2 H, d, J = 7.8 Hz, Ar*H*), 6.39 (1 H, d, J = 15.9 Hz, ArCH=C*H*), 4.20 (2 H, t, J = 6.0 Hz, (CH_2)$_3$$CH_3$), 2.37 (3 H, s, Ar$CH_3$), 1.73–1.63 (2 H, m, ($CH_2$)$_3$$CH_3$), 1.45–1.37 (2 H, m, ($CH_2$)$_3$$CH_3$), 0.96 (3H, t, J = 6.0 Hz, (CH_2)$_3$$CH_3$). δ_C (75 MHz, $CDCl_3$) 167.3, 144.6, 140.6, 131.7, 129.6, 128.0, 117.2, 64.4, 30.8, 21.5, 19.2, 13.7. HRMS (ESI) $[M]^+$ Calcd for $C_{14}H_{18}O_2$: 218.1307, found 218.1303.

Butyl-3-(4-methoxyphenyl)acrylate.[29,30] The product was obtained as a colorless oil. δ_H (300 MHz, $CDCl_3$) 7.64 (1 H, d, J = 15.9 Hz, ArC*H*=CH), 7.46 (2 H, d, J = 8.7 Hz, Ar*H*), 6.90 (2 H, d, J = 8.7 Hz, Ar*H*), 6.32 (1 H, d, J = 15.9, Hz, ArCH=C*H*), 4.19 (2 H, t, J = 6.9 Hz, (CH_2)$_3$$CH_3$), 3.82 (3 H, s, ArO$CH_3$), 1.73–1.64 (2 H, m, ($CH_2$)$_3$$CH_3$), 1.44 (2 H, q, J = 7.5 Hz, (CH_2)$_3$$CH_3$), 0.96 (3 H, t, J = 7.5 Hz, (CH_2)$_3$$CH_3$). δ_C NMR (75 MHz, $CDCl_3$): 167.4, 161.3, 144.2, 130.8, 127.2, 115.7, 113.3, 64.2, 55.3, 30.7, 19.2, 10.9 ; HRMS (ESI) $[M]^+$ Calcd for $C_{14}H_{18}O_3$: 234.1256, found 234.1260.

1,2-Diphenylethene.[29,30] The product was obtained as a colorless solid. δ_H (400 MHz, $CDCl_3$) 7.52 (4 H, d, J = 8.0 Hz, Ar*H*), 7.36 (4 H, t, J = 8.0 Hz, Ar*H*), 7.28–7.26 (2 H, m, Ar*H*), 7.11 (2 H, s, ArC*H*=C*H*). δ_C (100 MHz, $CDCl_3$) 137.3, 128.7, 127.6, 126.5; HRMS (ESI) $[M]^+$ Calcd for $C_{14}H_{12}$: 180.0939, found 180.0941.

1-Methyl-4-styrylbenzene.[29,30] The product was obtained as a colorless solid. δ_H (400 MHz, $CDCl_3$) 7.43 (2 H, d, J = 7.0 Hz, Ar*H*), 7.34 (2 H, d, J = 7.5 Hz, Ar*H*), 7.28 (2 H, t, J = 7.5 Hz, Ar*H*), 7.16 (2 H, d, J = 7.5 Hz Ar*H* and ArC*H*=CH), 7.09 (2 H, d, J = 7.0 Hz, Ar*H*), 7.02 (2 H, d, J = 7.5 Hz, Ar*H* and ArCH=C*H*), 2.30 (3 H, s, ArCH_3).

1-Methoxy-4-styrylbenzene.[29,30] The product was obtained as a colorless solid. δ_H (400 MHz, $CDCl_3$) 7.48 (4 H, dd, J = 8.0 and 12.0 Hz, Ar*H*), 7.35 (2 H, t, J = 8.0 Hz, Ar*H*), 7.26–7.22 (1 H, m, Ar*H*), 7.05 (2 H, q, J = 16.0 Hz, Ar*H*), 6.90 (2 H, d, J = 8.0 Hz, Ar*H*), 3.83 (3 H, s, ArOCH_3). δ_C (100 MHz, $CDCl_3$) 159.2, 137.6, 130.1, 128.6, 128.2, 127.7, 127.2, 126.6, 126.2, 55.3; HRMS (ESI) $[M]^+$ Calcd for $C_{15}H_{14}O$: 210.1045, found 210.1051.

4-Methoxy-4'-methylbiphenyl.[29,30] The product was obtained as a colorless solid. δ_H (400 MHz, $CDCl_3$) 7.52 (2 H, d, J =8.0 Hz, Ar*H*), 7.46 (2 H, d, J = 8.0 Hz, Ar*H*), 7.24 (2 H, d, J = 8.0 Hz, Ar*H*), 6.98 (2 H, d, J = 8.4 Hz, Ar*H*), 3.89 (3 H, s, ArOCH_3), 2.39 (3 H, s, ArCH_3). δ_C (100 MHz, $CDCl_3$) 159.1, 138.2, 136.6, 133.9, 129.6, 128.1, 126.8, 115.5, 114.3, 55.6, 21.3; HRMS (ESI) $[M]^+$ Calcd for $C_{14}H_{14}O$: 198.1045, found 198.1045.

4′-(4-Fluorobenzyloxy)-4-methylbiphenyl.[29,30] The product was obtained as a colourless needles. δ_H (300 MHz, $CDCl_3$) 7.44–7.31 (6 H, m, Ar*H*), 7.15 (2 H, d, J = 7.8, Ar*H*), 7.02–6.91 (4 H, m, Ar*H*), 4.96 (2 H, s, Ar*H*), 2.29(3 H, s, ArCH_3). δ_C (75 MHz, $CDCl_3$) 164.1, 160.9, 157.9, 137.8, 136.4, 134.1, 132.7, 129.4, 129.3, 129.2, 127.9, 126.6, 115.6, 115.3, 115.0, 69.4, 21.0; HRMS (ESI) $[M]^+$ Calcd for $C_{20}H_{17}FO$: 292.1263, found 292.1266.

1-Nitro-4-styrylbenzene.[29,30] The product was obtained as yellow solid. δ_H (400 MHz, $CDCl_3$) 8.21 (2 H, d, J = 8.8 Hz, Ar*H*), 7.62 (2 H, d, J = 8.7 Hz, Ar*H*), 7.54 (2 H, d, J = 7.5 Hz, Ar*H*), 7.36 (3 H, m, J = 27.1, 7.3 Hz, Ar*H,* ArC*H*=CH), 7.28 (1 H, d, J = 7.3 Hz, ArCH=C*H*), 7.13 (1 H, d, J = 16.3 Hz, Ar*H*).

1-Methoxy-4-(4-methylstyryl)benzene.[29,30] The product was obtained as a white solid. δ_H (400 MHz, $CDCl_3$) 7.43 (2 H, d, J =

8.7 Hz, Ar*H*), 7.38 (2 H, d, *J* = 8.1 Hz, Ar*H*), 7.15 (2 H, d, *J* = 8.0 Hz, Ar*H*), 7.02 (1 H, d, *J* = 16.3 Hz, ArC*H*=CH), 6.94 (1 H, d, *J* = 16.3 Hz, ArCH=C*H*), 6.89 (2 H, d, *J* = 8.7 Hz, Ar*H*), 3.82 (3 H, s, ArOCH_3), 2.35 (3 H, s, ArCH_3).

1-Chloro-4-(4-methoxystyryl)benzene.[29,30] The product was obtained as a colourless solid. δ_H (400 MHz, $CDCl_3$) 7.43 (2 H, d, *J* = 8.7 Hz, Ar*H*), 7.40 (2 H, d, *J* = 8.5 Hz, Ar*H*), 7.29 (2 H, d, *J* = 8.4 Hz, Ar*H*), 7.02 (1 H, d, *J* = 16.3 Hz, ArC*H*=CH), 6.95 – 6.83 (3 H, m, Ar*H,* ArCH=C*H*), 3.82 (3 H, s, ArOCH_3).

1-Chloro-4-styrylbenzene.[29,30] The product was obtained as colorless solid. δ_H (400 MHz, $CDCl_3$) 7.42 (2 H, d, *J* = 8.8 Hz, Ar*H*), 7.38 (2 H, d, *J* = 8.7 Hz, Ar*H*), 7.28-7.19 (5 H, d, Ar*H* and ArC*H*=CH), 7.03-6.94 (2 H, m, ArC*H* and ArCH=C*H*).

1-*tert*-Butyl-4-(4-chlorostyryl)benzene.[29,30] The product was obtained as colorless solid. δ_H (400 MHz, $CDCl_3$) 7.64-7.36 (6 H, m, *J* = 16.8, 7.4 Hz, Ar*H*), 7.29 (2 H, d, *J* = 8.7 Hz, Ar*H*), 7.05 (1 H, d, *J* = 16.4 Hz, ArC*H*=CH), 6.99 (1 H, d, *J* = 16.4 Hz, ArCH=C*H*), 1.32 (9 H, s, ArC(CH_3)$_3$).

Acknowledgments

RG acknowledges the financial support from the Council of Scientific & Industrial Research (CSIR) and the University of Delhi under the Scheme to Strengthen R&D. Authors thank CIF–USIC facility of this university for the crystallographic data collection and instrumental facilities; Dr. AK Verma for extending laboratory facilities; and Mr. Rakesh Kumar for some preliminary work. SK thanks CSIR for the RA fellowship.

Notes and references

[a]*Department of Chemistry, University of Delhi, Delhi – 110 007, India. Fax: +91-11-27666605; Tel: +91-11-27666646;*
E-mail: rgupta@chemistry.du.ac.in

† Electronic Supplementary Information (ESI) available: [Figures for the absorption, NMR spectra; and crystal structures and tables for NMR data, weak interactions, electrochemical data, and data collection and structure solution parameters]. See DOI: 10.1039/b000000x/

1 (a) A. L. Gavrilova and B. Bosnich, *Chem. Rev.,* 2004, **104**, 349; (b) I. Zilbermann, E. Maimon, H. Cohen and D. Meyerstein, *Chem. Rev.,* 2005, **105**, 2609.

2 (a) T. C. Harrop and P. K. Mascharak, *Coord. Chem. Rev.,* 2005, **249**, 3007; (b) D.-L.Popescu, A. Chanda, M. Stadler, F. Tiago de Oliveira, A. D. Ryabov, E. Munck, E. L. Bominaar and T. J. Collins, *Coord. Chem. Rev.,* 2008, **252**, 2050; (c) R. Ruiz, J. Faus, F. Lloret, M. Julve and Y. Journaux, *Coord.Chem. Rev.,* 1999, **193**, 1069; (d) P. K. Mascharak, *Coord. Chem. Rev.,* 2002, **225**, 201.

3 (a) T. J. Collins, *Acc. Chem. Res.,* 1994, **27**, 279; (b) T. J. Collins, *Acc. Chem. Res.,* 2002, **35**, 782; (c) A. Chanda, D-L. Popescu, F. T. de Oliveira, E. L. Bominaar, A. D. Ryabov, E. Munck and T. J. Collins, *J. Inorg. Biochem.,* 2006, **100**, 606; (d) D. W. Margerum, *Pure Appl. Chem.,* 1983, **55**, 23.

4 (a) E. Kimura, *J. Coord. Chem.,* 1986, **15**, 1; (b) E. Kimura, *Pure Appl. Chem.,* 1986, **58**, 1461; (c) G. De Santis, L. Fabbrizzi, M. Licchelli and P. Pallavicini, *Coord. Chem. Rev.,* 1992, **120**, 237; (d) L. Fabbrizzi, *Comments Inorg.Chem.,* 1985, ***4***, 33.

5 (a) S. K. Sharma, S. Upreti and R. Gupta, *Eur. J. Inorg. Chem.,* 2007, 3247; (b) S. K. Sharma, G. Hundal and R. Gupta, *Eur. J. Inorg. Chem.,* 2010, 621; (c) S. K. Sharma and R. Gupta, *Inorg. Chim. Acta,* 2011, **376**, 95; (d) J. Singh, G. Hundal and R. Gupta, *Eur. J. Inorg.Chem.,* 2008, 2052; (e) J. Singh, G. Hundal and R. Gupta, *Eur. J. Inorg. Chem.,* 2009, 3259; (f) J. Singh, G. Hundal, M. Corbella and R. Gupta, *Polyhedron*, 2007, **26**, 3893; (g) M. Munjal and R. Gupta, *Inorg. Chim. Acta*, 2010, **363**, 2734; (h) M. Munjal and R. Gupta, *Inorg. Chim. Acta,* 2011, **372**, 266; (i) M. Munjal, S. Kumar, S. K. Sharma and R. Gupta, *Inorg. Chim. Acta,* 2011, **377**, 144; (j) S. Kumar and R. Gupta, *Ind. J. Chem.,* 2011, **50A**, 1369; (k) S. Kumar, S. Vaidya, M. Pissas, Y. Sanakis, and R. Gupta, *Eur. J. Inorg. Chem.,* 2012, 5525; (l) S. Kumar, M. Munjal, J. Singh, and R. Gupta, *Eur. J. Inorg. Chem.,* 2014, 4957; (m) S. Kumar and R. Gupta, *Eur. J. Inorg. Chem.,* 2014, 5567.

6 (a) E. Negishi in *Handbook of Organopalladium Chemistry for OrganicSynthesis*; John Wiley & Sons, Hoboken, NJ, 2002; (b) P. M. Henry in *Palladium Catalyzed Oxidation of Hydrocarbons*, D. Reidel, Boston, 1980.

7 (a) K. Muniz, *Angew. Chem. Int. Ed.,* 2009, **48**, 9412; (b) A. J. Canty, *J. Chem. Soc., Dalton Trans.,* 2009, 10409; (c) T. W. Lyons and M. S. Sanford, *Chem. Rev.* 2010, **110**, 1147.

8 (a) T. Murahashi and H. Kurosawa, *Coord.Chem. Rev.,* 2002, **231**, 207; (b) C. Markert, M. Neuburger, K. Kulicke, M. Meuwly and A. Pfaltz, *Angew. Chem. Int. Ed.*, 2007, **46**, 5892; (c) T. Hama and J. F. Hartwig, *Org. Lett.,* 2008, **10**, 1545.

9 (a) D. C. Powers, M. A. L.Geibel, J. Klein and T. Ritter, *J. Am. Chem. Soc.,* 2009, **131**, 17050; (b) D. C. Powers and T. Ritter, *Nat. Chem.,* 2009, **1**, 302; (c) N. R. Deprez and M. S. Sanford, *J. Am. Chem. Soc.,* 2009, **131**, 11234.

10 (a) A. J. Blake, A. J. Holder, T. I. Hyde and M. Schroder, *J. Chem. Soc., Chem. Commun.,* 1987, 987; (b) A. J. Blake, L. M. Gordon, T. I. Hyde, G. Reid and M. Schroder, *J. Chem. Soc., Chem. Commun.,* 1988,1452.

11 J. R. Khusnutdinova, N. P. Rath and L. M. Mirica, *J. Am. Chem. Soc.,* 2010, **132**, 7303.

12 W. J. Geary, *Coord. Chem. Rev*., 1971, **7**, 81.

13 K. Nakamoto in *Infrared and Raman Spectra of Inorganic and Coordination Compounds*, John Wiley & Sons, 1986.

14 S. P. Gavrish, Y. D. Lampeka, H. Prtizkow and P. Lightfoot, *Dalton Trans.,* 2010, **39**, 7706.

15 (a) Y. D. Lampeka, S. P. Gavrish, R. W. Hay, T. Eisenblatter and P. Lightfoot, *J. Chem. Soc., Dalton Trans.,* 2000, 2023; (b) S. P. Gavrish, Y. D. Lampeka and P. Lightfoot, *Inorg. Chim. Acta*, 2004, **357**, 1023.

16 L. Yang, D. R. Powell and R. P. Houser, *Dalton Trans.,* 2007, 955.

17 (a) N. Miyaura, K. Yamada and A. Suzuki, *Tetrahdron Lett.* 1979, **20**, 3437; (b) N. Miyaura and A. Suzuki, *Chem. Rev.,* 1995, **95**, 2457.

18 R. F. Heck and J. P. Nolley Jr., *J. Org. Chem.,* 1972, **37**, 2320.

19 (a) A. R. Dick, J. W. Kampf and M. S. Sanford, *J. Am. Chem. Soc.,* 2005, **127**, 12790; (b) A. J. Canty, *Acc. Chem. Res.,* 1992, **25**, 83.

20 (a) F. E. Hahn, M. C. Jahnke, V. Gomez-Benitez, D. Morales-Morales, T. Pape, *Organometallics*, 2005, **24**, 6458; (b) S. Oi, K. Sakai, Y. Inoue, *Org. Lett.* 2005, **7**, 4009; (c) F. E. Hahn, M. C. Jahnke, T. Pape, *Organometallics*, 2006, **25**, 5927.

21 G. H. Whitesides, M. Hackett, R. L. Brainard, J.-P. P. M. Lavalleye, A. F. Sowinski, A. N. Izumi, S. S. Moore, D. W. Brwon, E. M. Staudt, *Organometallics*, 1985, **4**, 1819.

22 An additional experiment was performed wherein complex **2** was used for the Heck coupling reaction between iodobenzene and styrene. In this reaction, "four" consecutive batches of iodobenzene and styrene were added within the same reaction vessel containing complex **2** and in all four cases; complete transformation was noted. Importantly, for each independent cycle the product transformation remained constant: a = b = c = d (see Figure S9, ESI).

23 D. D. Perrin, W. L. F. Armarego and D. R. Perrin in *Purification of Laboratory Chemicals*, Pergamon Press, Oxford, 1980.

24 N. G. Connely and W. E. Geiger, *Chem. Rev.,* 1996, **96**, 877.

25 CrysAlisPro, Oxford Diffraction Ltd. Version 1.171.33.4pb, 2009.

26 A. Altomare, G. Cascarano, C. Giacovazzo, A. Guagliardi, *J. Appl. Crystallogr.* **1993**, *26*, 343.

27 G. M. Sheldrick, *Acta Crystallogr., Sec. A* **2008**, *64*, 112.

28 J. Farrugia, WinGX version 1.64, An Integrated System of Windows Programs *for the Solution, Refinement and Analysis of Single-Crystal X-rayDiffraction Data;* Department of Chemistry, University of Glasgow, 2003.

29 H. F. Sore, C. M. Boehner, S. J. F. MacDonald, D. Norton, D. J. Fox, D. R. Spring, *Org. Biomol. Chem.*, 2009, **7**, 1068.

30 B. Schmidt, N. Elizarov, R. Berger, F. Hölter, *Org. Biomol. Chem.*, 2013, **11**, 3674.